Studies of W(-> e nu) boson production in pp interactions in the ATLAS experiment

D. Tsionou

Studies of $W(\rightarrow e\nu)$ boson production in pp interactions in the ATLAS experiment

Dimitra TSIONOU
Laboratoire d' Annecy-le-Vieux de Physique des Particules
& University of Sheffield

Résumé

Cette note porte sur l'étude de la production des bosons W avec l'expérience ATLAS dans les interactions proton-proton à l'énergie de 7 TeV dans le centre de masse. Des critères de sélection des événements $W \rightarrow e\nu$ sont explorés ainsi que le développement d'une méthode permettant d'estimer les contributions du bruit de fond QCD.

1.1 W Physics and Parton Density Functions

At leading order (LO), W production occurs via the process $q\bar{q} \rightarrow W$. The momentum fractions of the two participating partons with respect to the initial proton are given by

$$x_1 = \frac{M_W}{\sqrt{s}} e^{y} \text{ and } x_2 = \frac{M_W}{\sqrt{s}} e^{-y}$$

where M_W is the centre of mass energy of the hard scattering ($\hat{s} = Q^2 = M_W^2$), $\sqrt{s}$ is the centre of mass energy of the proton-proton collision ($\sqrt{s} = 7$ TeV at the LHC) and $y = \frac{1}{2} ln \frac{E + p_l}{E - p_l}$ the W rapidity.

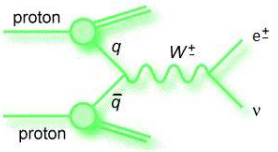

Parton density functions (PDFs) are defined as the probability of finding a parton (valence quark, sea quark or gluon) with a momentum fraction x at momentum transfer Q^2 within the proton. Perturbative QCD provides the evolution for the parton densities as functions of Q^2 (DGLAP equations) but not their analytic forms as functions of x. However, by extrapolating the structure functions from one (x, Q^2) to a different (x', Q'^2) we also extrapolate their errors. This results in large errors for the PDFs at non-measured (x, Q^2) regions. [1]

At the Large Hadron Collider an asymmetry in the production rate of W^+ $(u\bar{d})$ and W^- $(\bar{u}d)$ is expected since it is a proton-proton collider. The W asymmetry can be defined as

$$A_W = \frac{\frac{d\sigma_+}{d\eta_e} - \frac{d\sigma_-}{d\eta_e}}{\frac{d\sigma_+}{d\eta_e} + \frac{d\sigma_-}{d\eta_e}}$$

where ${}^{d\sigma^{\pm}}/_{d\eta_e}$ is the differential cross-section of $W^{\pm}$ in bins of the pseudorapidity of the electron of the decay process. The W differential cross-section measurements as well as the W asymmetry can be used to constrain the parton density functions and provide information on the u and d quark PDFs for the low x-region probed at LHC. An advantage of the W asymmetry measurement is that the uncertainty from the gluon PDF cancels out.

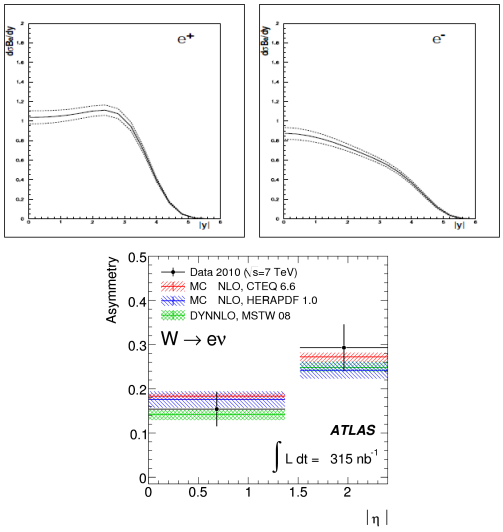

FIG. 1.1 – Top left plot : e^+ decay rapidity spectrum from CTEQ6.1 PDFs; top right plot : e^- decay rapidity spectrum from CTEQ6.1 PDFs [2] ; bottom plot : electron charge asymmetry as measured with the first 315 nb^{-1} ATLAS data. Several theoretical predictions are superimposed [3]

1.2 Experimental Setup

1.2.1 LHC and ATLAS

During the proton runs (April-November 2010) of the Large Hadron Collider (LHC), ATLAS has collected approximately 50 pb^{-1} of data at the centre of mass energy $\sqrt{s} = 7$ TeV.

The ATLAS detector is a general multi-purpose detector and as such it consists of an Inner Detector (used for tracking), an Electromagnetic and a Hadronic Calorimeter (for energy reconstruction) and a Muon Detector (for muon identification).

The following subsection will describe the Liquid Argon (LAr) calorimeter since it plays an important role in electron detection.

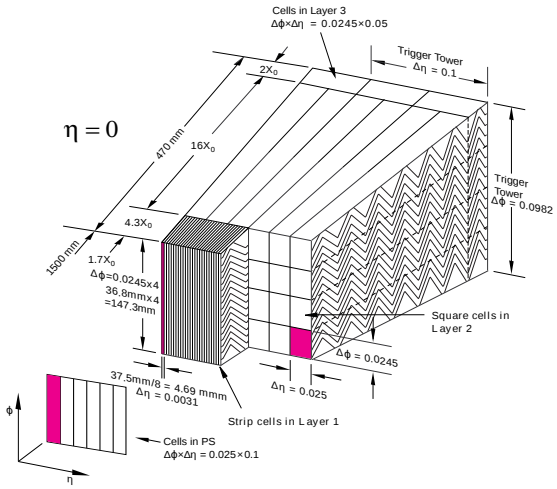

FIG. 1.2 – The accordion and sampling structure of the EM Barrel Calorimeter showing the difference in granularity between the different samplings. Its longitudinal segmentation allows to look at the shower development [4]

1.2.2 Electromagnetic Calorimeter and Digital Signal Processor

The ATLAS Liquid Argon Electromagnetic (EM) Calorimeter allows to reconstruct and identify the electrons and photons produced in each collision and to measure their energy and position. It is a lead – liquid argon accordion-shaped sampling detector which consists of approximately 200,000 electronic channels. There are 4 Liquid Argon sub-detectors in ATLAS : the EM barrel, the EM end-cap, the hadronic end-cap (HEC) and the forward calorimeter (FCAL).

The DSP (Digital Signal Processor) is a part of the processing units which are housed on the Read-Out Drivers, an important part of the back-end electronics. The DSP computes the energy, signal timing and a quality factor for each detector cell. In this way, it is possible to store directly high level information (cell energy and time) rather than all the digital samples composing the electric signal recorded when a particle crosses the detector.

The energy is calculated for every LAr cell while there is a threshold for the time and quality factor computation. Taking into account both the precision of the measurement and the performance of the DSP, 4 energy ranges are defined, each one with a different precision.

The DSP plays an important role since the energy reconstruction of the electrons is based on the cell energy computation that takes place on the DSP.

Energy range	Energy $[MeV]$	ΔE $[MeV]$
1^{st}	$E < 2^{13}$	1
2^{nd}	$2^{13} < E < 2^{16}$	8
3^{rd}	$2^{16} < E < 2^{19}$	64
4^{th}	$2^{19} < E < 2^{22}$	512

TAB. 1.1 – Precision of the DSP for the four different energy ranges defined

1.3 $W \rightarrow e\nu$ Analysis

1.3.1 Electron Identification and Isolation

Several variables are used to identify electrons and to distinguish them from background particles (such as hadrons, pions and photon conversions). In ATLAS there are three levels of identification - loose, medium and tight - that include calorimetric cuts (lateral and longitudinal shower shapes) as well as track-matching cuts all set in a p_T and η grid.

Another powerful variable to select $W \rightarrow e\nu$ events is the calorimetric isolation. Isolation variables represent the activity around the object we are interested in. We expect the electron coming from the W to be isolated while the background electron candidates from QCD processes are not. This is because of the fact that this QCD background is due to jets faking electrons or electrons from hadron decays that are in jets.

1.3.2 Event Selection

The selection criteria for $W \rightarrow e\nu$ events include event cleaning, electron and E_T^{miss}, m_T^W cuts.

The event selection cuts require events that have passed an appropriate trigger and have at least one good reconstructed vertex.

The electron cuts include the kinematic criteria :

- transverse momentum $p_T > 20\ GeV$ and
- pseudorapidity up to $|\eta| < 2.5$ (excluding the crack region of the detector between the barrel and the end-cap)

In addition, tight identification is applied in order to distinguish between electrons and other particles.

Since the ν escapes the detection, there is missing transverse energy in W events. The cut on the E_T^{miss} ($E_T^{miss} > 25\ GeV$) is a powerful cut in this case. Lastly, a cut on the transverse mass of the W ($m_T^W > 40\ GeV$) is used in order to have a cleaner sample.

After all these selection criteria, a clean sample is obtained where the signal to background ratio is $S/B \approx 15$.

1.3.3 Electron Shower Shapes

$W \rightarrow e\nu$ is a clean signal therefore the selected events can be used to compare the calorimetric response of electrons in data and Monte Carlo. Since the above described analysis contains calorimetric cuts, we have developed alternative selection criteria in order to study

the longitudinal and lateral shower shapes of the e from the W decay. In this method, the electron selection relies mostly on Inner Detector variables rather than calorimetric ones.

More precisely in this analysis, the same cuts on the momentum, missing transverse energy and transverse mass are applied but instead of the e tight identification, loose identification is used. In addition, we require a minimum number of hits for each sub-detector of the ATLAS Inner Detector and that the electron is isolated.

In Figure 1.3 a slight discrepancy between data and Monte Carlo can be seen on the width of the electromagnetic shower as well as on the E/p ratio. As far as the width of the shower is concerned, part of the effect is due to a simplification on the description of the LAr electrodes on the Monte Carlo. Further investigation is ongoing to fully understand this discrepancy. The difference on the plot of the E/p ratio is due to a calibration effect.

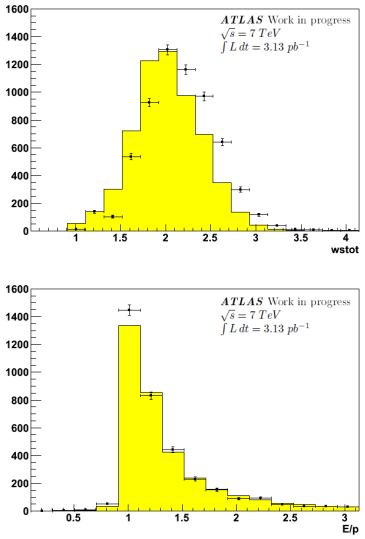

FIG. 1.3 – The top figure shows the width of the electromagnetic shower. The shower width is broader on the data in comparison to the Monte Carlo ; The bottom picture shows the ration E/p. The reason for this discrepancy is explained on the text

1.4 Background Estimation

In order to compute the W cross-section, the number of background events has to be evaluated. There are two different sources of background for the $W \to e\nu$ channel. One is the QCD background and the other includes electroweak processes. While the electroweak processes are fairly well-known, the QCD background needs to be determined with (semi)data-driven methods.

1.4.1 Electroweak Background

The electroweak processes contributing to the $W \to e\nu$ background are mainly the $Z \to ee$ and $W \to \tau\nu$. Since they are fairly well-known (the uncertainty on $\sigma \cdot BR$ is of the level of 5% for both processes), in order to study their effect on the signal Monte Carlo generated samples are used. After all the selection cuts are applied, the $Z \to ee$ contribution is negligible (only 3 ‰) while $W \to \tau\nu$ is the most significant electroweak background as it amounts to 2.5% of the signal.

1.4.2 QCD Background Estimation

In this study we use the following method to estimate the QCD background. The number of candidate events after the analysis is

$$N_{Wcand} = N_W + N_{QCD} \tag{1.1}$$

and by adding an additional cut

$$N^{cut}_{Wcand} = \epsilon_{sig} \cdot N_W + \epsilon_{QCD} \cdot N_{QCD} \tag{1.2}$$

From the equations 1.1 and 1.2 the necessary quantities to measure in order to calculate the number of QCD candidates N_{QCD} are :

- the numbers of W candidate events before and after the additional cut N_{Wcand} and N^{cut}_{Wcand} obtained from the cut-flow of our analysis,
- the signal efficiency ϵ_{sig} measured on $Z \to ee$ events using Tag&Probe and
- the QCD efficiency ϵ_{QCD}.

To measure the ϵ_{QCD}, it is essential to select a signal-free QCD sample which is similar to the one that passes the $W \to e\nu$ selection criteria.

Once all these quantities are measured, the N_{QCD} can be calculated using the following formula

$$N_{QCD} = \frac{\epsilon_{sig} \cdot N_{Wcand} - N^{cut}_{Wcand}}{\epsilon_{sig} - \epsilon_{QCD}} \tag{1.3}$$

The additional cut that is used in this study is the electron calorimetric isolation.

1.4.3 QCD Background Sample

As mentioned previously in order to measure the ϵ_{QCD} it is necessary to select a QCD sample similar to the signal. For this reason the same cuts as in the $W \to e\nu$ analysis are applied with the exception of using e medium identification instead of tight and reversing the E_T^{miss} cut.With this method, a signal-free QCD sample is indeed selected (only 3% contamination from the electroweak processes $Z \to ee$, $W \to e\nu$ and $W \to \tau\nu$).

After selecting the background sample and applying the additional isolation cut, the efficiency of the isolation cut ϵ_{QCD} can be measured on this QCD sample.

N_{Wcand}	N^{cut}_{Wcand}	ϵ_{sig}	ϵ_{QCD}
9901 ± 100	9522 ± 98	0.984 ± 0.006	0.491 ± 0.002

TAB. 1.2 – Quantities used in the N_{QCD} calculation and their corresponding values

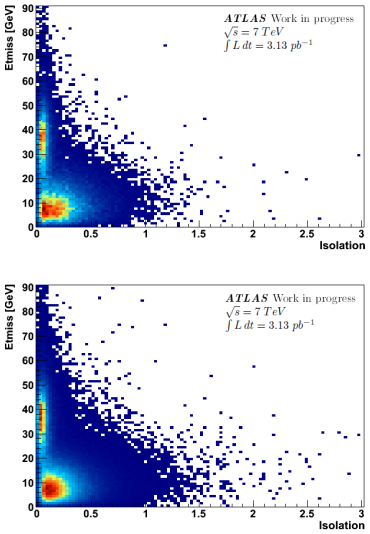

FIG. 1.4 – The top plot shows the E_T^{miss} vs electron isolation distribution for the $W \rightarrow e\nu$ candidates in data while the bottom plot shows the same distribution for the QCD sample we have selected and $W \rightarrow e\nu$ Monte Carlo. It is apparent that there is a similar correlation in both samples

Using the numbers shown on Table 1.2 and the formula 1.3, we can calculate the number of QCD events $N_{QCD} = 447 \pm 120(\text{stat})$. This result is in agreement with other methods.

1.5 Conclusions

In this note, two alternative methods for selecting $W \rightarrow e\nu$ events have been studied, both providing a good S/B ratio. One of these gives us the opportunity to study the electron calorimetric shower shapes thus providing useful information on the understanding of the detector response.

Furthermore, two different sources of background for this process have been studied : the electroweak and the QCD background. For the electroweak we rely on the Monte Carlo description while we have developed a data-driven method to estimate the amount of QCD background.

Références

[1] A.Tricoli, Parton Densities at the LHC (arXiv :hep-ex/0808.2579v1)

[2] A.M.Cooper-Sarkar, Low-x physics and W and Z production at the LHC (arXiv :hep-ph/0512228v1)

[3] The ATLAS Collaboration, Measurement of the $W \rightarrow l\nu$ and $Z/\gamma^* \rightarrow ll$ production cross sections in proton-proton collisions at $\sqrt{s} = 7$ TeV with the ATLAS detector (arXiv :1010.2130v1)

[4] ATLAS Collaboration. ATLAS Calorimeter Performance. Technical report, 1997